

# Actinide Topological Insulator Materials with Strong Interaction

Xiao Zhang<sup>1</sup>, Haijun Zhang<sup>1</sup>, Claudia Felser<sup>2</sup>, Shou-Cheng Zhang<sup>1</sup>

<sup>1</sup>*Department of Physics, McCullough Building, Stanford University, Stanford, California 94305-404531*

<sup>2</sup>*Institut für Anorganische Chemie und Analytische Chemie, Johannes Gutenberg - Universität, 55099 Mainz, Germany \**

Topological band insulators have recently been discovered in spin-orbit coupled two and three dimensional systems. In this work, we theoretically predict a class of topological Mott insulators where interaction effects play a dominant role. In actinide elements, simple rocksalt compounds formed by Pu and Am lie on the boundary of metal to insulator transition. We show that interaction drives a quantum phase transition to a topological Mott insulator phase with a single Dirac cone on the surface.

Topological insulators are new states of quantum matter with a full insulating gap in the bulk and gapless Dirac fermion states on the surface[1–3]. Spin-orbit coupling plays a dominant role in topological band insulators HgTe, Bi<sub>1-x</sub>Sb<sub>x</sub> and Bi<sub>2</sub>Te<sub>3</sub> class of materials. The basic mechanism for all topological insulators discovered so far is the band inversion driven by spin-orbit coupling[4]. Soon after the discovery of topological band insulators, the concept of a topological Mott insulator has been proposed theoretically[5], where interaction effects are responsible for topological insulating behavior. The interplay between electron interaction and spin-orbit coupling could enhance the bulk insulating gap, which is important for device applications. Magnetic and superconducting order driven by interactions could co-exist with topological order, and give rise to exotic excitations such as magnetic monopole[6], Majorana fermion[7] and dynamic axion field[8].

In this work we theoretically predict a new class of topological Mott insulators in actinide compounds with electrons in the 5f valence orbitals. Interaction and spin-orbit coupling energy scales are comparable in these compounds, making them ideal material systems to investigate the interplay between these two important effects. Simple rocksalt compounds formed by Pu and Am lie on the boundary of metal to insulator transition, where the 5f electrons change from itinerant to localized characters[9]. Using AmN as an example, we show that this rocksalt compound is metallic without interactions, but an insulating gap is induced by interactions. A band inversion between the 6d and the 5f drives the system into a topological insulator phase with a single Dirac cone on the surface. The predicted actinide topological insulators are binary compounds with a simple rocksalt crystal structure and reasonably large energy gaps, providing an ideal platform to investigate interacting topological insulators. Standard topological band insulators in the Bi<sub>2</sub>Te<sub>3</sub> class of materials have bulk carriers induced by disorder. In contrast, the actinide compounds predicted in this work have stronger three dimensional ionic bonds. As a result, they may have fewer bulk de-

fects; in fact, earlier photo-emission experiments indicate vanishing density of states at the fermi level[10].

Americium and plutonium are actinide elements with electron configurations of  $5f^76d^07s^2$  and  $5f^66d^07s^2$ . Many of the Am mono-pnictides AmX (X=N, P, As, Sb, and Bi) and Pu mono-chalcogenides PuY (Y=Se and Te) are known to be nonmagnetic and narrow-gap semiconductors[10–15]. At ambient conditions, they crystallize in the rocksalt structure. The rocksalt structure has face-centered cubic (FCC) symmetry with  $Fm\bar{3}m$  space group, shown in Fig. 1A with AmN as an example. It can be represented as two interpenetrating FCC lattices with a two-atom basis. The first atom (Am) is located at each lattice point, and the second atom (N) is located half way between lattice points along the FCC unit cell edge. The bravais lattice vectors are  $a_1 = (0, a/2, a/2)$ ,  $a_2 = (a/2, 0, a/2)$  and  $a_3 = (a/2, a/2, 0)$ . Its Brillouin zone (BZ) has three independent time-reversal-invariant-momentum (TRIM) points, which are  $\Gamma(000)$ ,  $X(\pi\pi0)$  and  $L(\pi00)$  as shown in Fig. 1B.

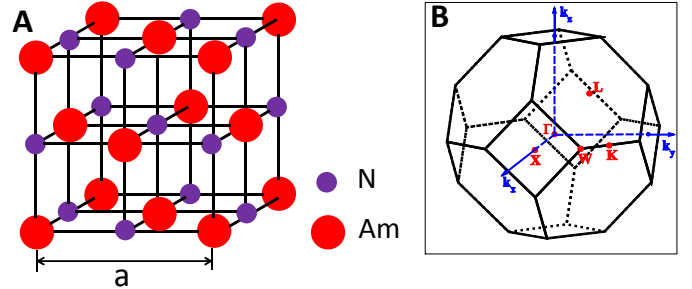


FIG. 1. Crystal structure and Brillouin zone. (A) Rocksalt crystal structure of AmN with  $Fm\bar{3}m$  space group. Am and N separately form a face-centered cubic (fcc) sub-lattice, and these two sub-lattices are at a distance of  $a/2$  away with each other along one cubic edge. (B) Brillouin zone for AmN of rocksalt structure. It has three independent time-reversal-invariant points are  $\Gamma(000)$ ,  $L(\pi00)$ , and  $X(\pi\pi0)$ .

In order to study the electronic structure of these materials, *ab-initio* calculations are carried out in the framework of local density functional approximation (LDA)

\* sczhang@stanford.edu.

supported by BSTATE package [16] within the plane-wave pseudo-potential method. The ultra-soft pseudo-potential[17] is employed for localized orbitals, i.e., Am(Pu) 5f and N 2p orbitals. The  $\mathbf{k}$ -point grid is taken as  $16 \times 16 \times 16$  and the kinetic energy cutoff is fixed to 340eV for all the self-consistent calculations. The spin-orbit coupling (SOC) interaction is taken into account because both Am and Pu have very heavy nuclei. Due to the localization of 5f electrons, LDA+U method[18] is used to deal with strong correlations in these compounds with  $U = 2.5\text{eV}$  for Am [11] and  $U = 3.0\text{eV}$  for Pu[13]. We use the experimental lattice constants in our calculations[19].

Because all the AmX and PuY have similar electronic structures, here AmN is taken as an example. The band structures for AmN with  $U = 0\text{eV}$  and  $U = 2.5\text{eV}$  are shown in Fig. 2A-B separately. The strong interaction  $U$  is responsible for the metal to insulator transition. If we ignore the effect of  $U$  in the calculation, there are residual 5f states at the Fermi level ( $E_F$ ), indicating metallic behavior (Fig. 2A). Only by taking into count of  $U = 2.5\text{eV}$ , those residual 5f states are lifted away from  $E_F$ , and we can correctly predict AmN to be an insulator (Fig.2 B), consistent with the experimental finding[10]. We will elaborate this point in the following energy band analysis. First of all, we consider the Am-X (Pu-Y) bonding. One  $f$  and two  $s$  electrons of Am bond with the three  $p$  electrons of pnictides, while two  $s$  electrons of Pu bond with the four  $p$  electrons of chalcogenides. As a result, there are six  $f$  electrons left in the ground states for both AmX and PuY before we consider the hybridization between 5f and 6d states in Am or Pu. Since these strong bonding states are further away from  $E_F$  than the low energy Am-Am and Pu-Pu bonding states, we ignore them in our band structure analysis in Fig. 3. In the following we will just consider the Am-Am and Pu-Pu  $d$  and  $f$  low energy bonding states. The 6d orbital first splits into  $e_g$  and  $t_{2g}$  states due to the large crystal-field splitting (CFS) and then splits again into  $\Gamma_7^+$  and  $\Gamma_8^+$  subbands due to a small spin-orbit coupling (SOC) (Fig. 3)[20]. The  $f$  states split into  $5f^{5/2}$  and  $5f^{7/2}$  states with angular momentum of 5/2 and 7/2, due to the SOC interaction. For the  $U = 2.5\text{eV}$  case, the Coulomb  $U$  additionally shifts the  $5f^{7/2}$  states away from  $E_F$ [11], leading to the metal to insulator transition (Fig. 2A-B). Therefore, only the  $5f^{5/2}$  states are fully occupied with the six  $f$  electrons with a non-magnetic ground state, before hybridizing with  $d$  orbital. CFS further splits the  $5f^{5/2}$  states into  $\Gamma_8^-$  and  $\Gamma_7^-$  [21].

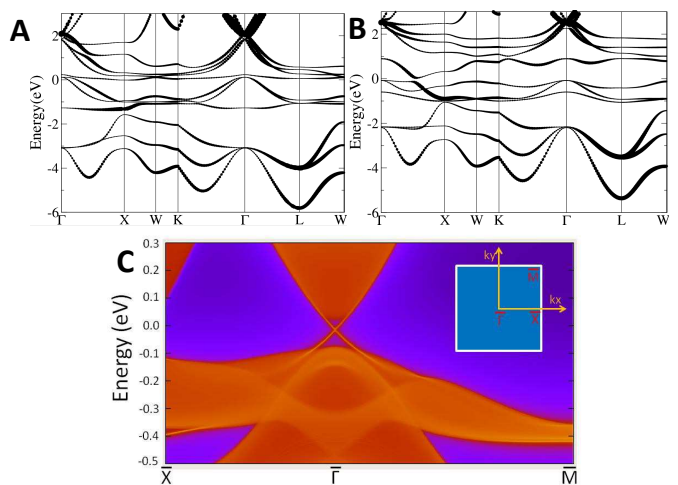


FIG. 2. Band structure and topological surface states. Band structures for AmN at (A)  $U = 0\text{eV}$  and (B)  $U = 2.5\text{eV}$ . The line width in these fat band structures corresponds to the projected weight of Am's d orbitals on Bloch states. The f states are divided into two parts with angular momentum 5/2 and 7/2 due to the spin-orbit-coupling interaction. The part with angular momentum 5/2 is occupied, and the other part with angular momentum 7/2 is partially occupied with  $U = 0\text{eV}$ . For  $U = 2.5\text{eV}$  case, these partially occupied f states of angular momentum 7/2 move further toward high energy and become completely unoccupied. (C) Energy spectrum of the *ab-initio* calculation based TB hamiltonian with the open boundary condition along '+z' direction. One surface Dirac cone is clearly seen at  $\Gamma$  point as red lines dispersing in the bulk gap on the AmN [001] surface. In the inset, the projected two dimension BZ is shown.

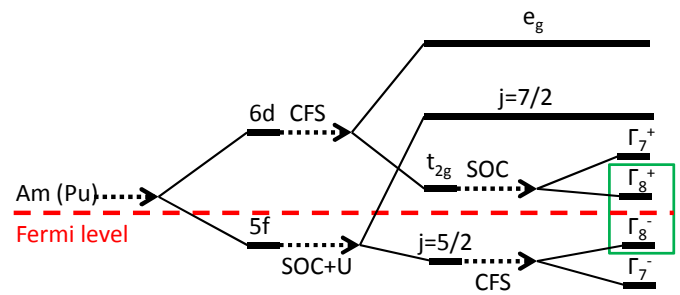


FIG. 3. Band sequence. Schematic diagram of the evolution from the atomic d/f orbitals of Am or Pu into the conduction and valence bands of AmX or PuY at the  $\Gamma$  point. The black dashed arrow represent the effect of turning on of chemical bonding, CFS, SOC and  $U$  (see text). The red dashed line represents the Fermi energy. The low energy bands in the green box explains the topological physics.

At  $E_F$ , the most important feature is the downward dispersion of the  $\Gamma_8^+$  subband of Am's d band, it crosses the  $\Gamma_8^-$  subband of the  $5f^{5/2}$  bands along  $\Gamma - X$  direction, leading to a band inversion near the  $X$  point in

	$E_g$	$\Gamma$	3X	4L	Tot.
AmN	0.100eV	-	+	-	-
AmP	0.085eV	-	+	-	-
AmAs	0.080eV	-	+	-	-
AmSb	0.055eV	-	+	-	-
AmBi	0.040eV	-	+	-	-
PuSe	0.2eV	-	+	-	-
PuTe	0.178eV	-	+	-	-

TABLE I. Energy gap and parity eigenvalue.  $E_g$  indicates the energy gap.  $\Gamma$ ,  $X$  and  $L$  are the time-reversal-invariant (TRIM) points in Brillouin zone. '-' and '+' indicate the 'odd' and 'even' parity product for all the occupied bands. 'Tot.' means the total parity product of all TRIM points.

the BZ (Fig. 3). A energy gap is formed at the crossing point due to the f-d hybridization. Because the d and f orbitals have 'even' and 'odd' parities at three  $X$  points, this inversion of bands with opposite parity signs determines the non-trivial topology of these materials. This d-f band inversion phenomenon is a generalization of the band inversion between the s and p bands in HgTe quantum wells[4] and between p bands of opposite parities in Bi<sub>2</sub>Te<sub>3</sub> class of materials [22]. We calculate the parity at all TRIM points[23] (Table 1) and predict that AmN and all other AmX materials in this family are non-trivial topological insulators with their band gaps shown in Table 1. The LDA+U method cannot obtain a energy gap for PuTe, which was measured experimentally to be 0.2eV at ambient pressure and 0.4eV with pressure up to 5 GPa[13, 14]. Suzuki and Oppeneer employ dynamical mean-field theory (DMFT) method and successfully reproduce the energy gap for PuSe and PuTe[13, 15]. With the same low energy physics as AmN, we can conclude that PuSe and PuTe are non-trivial TIs.

According to the *ab-initio* calculation, the two low energy  $\Gamma_8^\pm$  bands can capture the salient topological features of these materials. Therefore, we propose the following  $8 \times 8$  Hamiltonian:

$$H = \begin{pmatrix} H_d & H_{df} \\ H_{df}^\dagger & H_f \end{pmatrix} \quad (1)$$

$H_d$  and  $H_f$  are  $4 \times 4$  Hamiltonian for  $\Gamma_8^+$  and  $\Gamma_8^-$  representations with an effective angular momentum  $j = 3/2$ . We first write down the continuum Hamiltonian near the  $\Gamma$  point of the BZ and then extend it to a tight binding (TB) model for the full BZ. The effective Hamiltonian for  $\Gamma_8^\pm$  bands is the Luttinger model [24]:

$$H_{d(f)} = C_{d(f)} + A_{d(f)}k^2 + B_{d(f)}(k \cdot J_{3/2})^2 + D_{d(f)}(k_x^2(J_{3/2}^x)^2 + k_y^2(J_{3/2}^y)^2 + k_z^2(J_{3/2}^z)^2) \quad (2)$$

$A_{d(f)}, B_{d(f)}, C_{d(f)}, D_{d(f)}$  are constants and  $J_{3/2}$  are spin matrices for angular momentum 3/2. The first three terms have continuous rotational symmetry; the last term breaks continuous rotational symmetry while preserving cubic symmetry, which is responsible for the band inversion only along  $\Gamma - X$  direction rather than other directions in the BZ[25]. The off-diagonal Hamiltonian  $H_{df}$  connects  $d$  and  $f$  bands of opposite parities, therefore, the first order term can be written as  $H_{df} = F(k \cdot J_{3/2})$  with continuous rotational symmetry,  $F$  again is a parameter.

Because the  $5f$  and  $6d$  orbitals are localized, we consider only the nearest neighborhood hopping of Am-Am and Pu-Pu atoms. Each Am (Pu) atom has twelve nearest neighbors located at  $\pm a_1, \pm a_2, \pm a_3, \pm(a_2 - a_1), \pm(a_2 - a_3)$  and  $\pm(a_3 - a_1)$ . So we can extend the above continuum model to the TB lattice model and reproduce the low energy bands of these materials well, with AmN as an example[25]. Besides this single particle part, our Hamiltonian also includes the on-site interaction parameter  $U$  for electrons on the f orbital. One important effect the  $U$  interaction is to renormalize the parameters of the single particle Hamiltonian, and to induce a metal-insulator transition. On the insulator side, we can effectively fit our model with renormalized parameters to the first-principle calculations.

To observe the surface states, we construct a *ab-initio* calculation for the semi-infinite AmN system with open boundary condition in '+z' direction on the basis of maximally localized Wannier functions (MLWFs)[26, 27]. We can obtain the surface Green's function of the semi-infinite system iteratively. Finally the local density of states(LDOS) can be calculated with the imaginary part of these Green's functions. From these LDOS, we can obtain the dispersion of the surface states, shown in Fig. 2C. A single Dirac cone at  $\bar{\Gamma}$  clearly shows up in the energy gap, which demonstrates the non-trivial  $Z_2$  topology of the material in addition to the parity analysis. The Fermi-velocity for the Dirac cone is  $v_F \simeq 1.3 \times 10^5 m/s$ , a little smaller than Bi<sub>2</sub>Se<sub>3</sub>[22]. To confirm this result, we also take open boundary condition in  $z$  direction in the analytical TB model (1)[25], from which we have observed the same single surface state Dirac cone at  $\Gamma$  point of the BZ as in the *ab-initio* calculation based TB Hamiltonian.

## ACKNOWLEDGMENTS

We would like to thank Dr. Sri Raghu for useful discussions. This work is supported by the ARO with grant number W911NF-09-1-0508.

- 
- [1] X. L. Qi and S. C. Zhang, Phys. Today **63**, 33 (2010).
- [2] X. L. Qi and S. C. Zhang, Rev. Mod. Phys. **83**, 1057 (2011).
- [3] M. Z. Hasan and C. L. Kane, Rev. Mod. Phys. **82**, 3045 (2010).
- [4] B. A. Bernevig, T. L. Hughes, and S.C. Zhang, Science **314**, 1757 (2006).
- [5] C. H. S. Raghu, Xiao-Liang Qi and S.-C. Zhang, Phys. Rev. Lett. **100**, 156401 (2008).
- [6] J. Z. S.-C. Z. Xiao-Liang Qi, Rundong Li, Science **323**, 1184 (2009).
- [7] C. L. K. Liang Fu, Phys. Rev. Lett. **100**, 096407 (2008).
- [8] R. Li, J. Wang, X. Dai, and S.-C. Zhang, Nat. Phys. **6**, 284 (2010).
- [9] K. T. Moore and G. van der Laan, Rev. Mod. Phys. **81**, 235 (2009).
- [10] T. Gouder, P. M. Oppeneer, F. Huber, F. Wastin, and J. Rebizant, Phys. Rev. B **72**, 115122 (2005).
- [11] D. B. Ghosh, S. K. De, P. M. Oppeneer, and M. S. S. Brooks, Phys. Rev. B **72**, 10800 (1992).
- [12] S. Suzuki and T. Ariizumi, J. Phys. Soc. Jpn. **76**, 024707 (2007).
- [13] M.-T. Suzuki and P. M. Oppeneer, Phys. Rev. B **80**, 161103 (2009), URL <http://link.aps.org/doi/10.1103/PhysRevB.80.161103>.
- [14] V. Ichas, J. C. Griveau, J. Rebizant, and J. C. Spirlet, Phys. Rev. B **63**, 045109 (2001).
- [15] M. S. S. Brooks, J. Magn. Magn. Mater. **63-64**, 649 (1987).
- [16] Z. Fang and K. Terakura, Journal of Physics: Condensed Matter **14**, 3001 (2002).
- [17] D. Vanderbilt, Phys. Rev. B **41**, 7892 (1990), URL <http://link.aps.org/doi/10.1103/PhysRevB.41.7892>.
- [18] V. I. Anisimov, I. V. Solovyev, M. A. Korotin, M. T. Czyżyk, and G. A. Sawatzky, Phys. Rev. B **48**, 16929 (1993), URL <http://link.aps.org/doi/10.1103/PhysRevB.48.16929>.
- [19] F. Wastin, J. Spirlet, and J. Rebizant, Journal of Alloys and Compounds **219**, 232 (1995), ISSN 0925-8388.
- [20] M. S. Dresselhaus, G. Dresselhaus, and A. Jorio, *Group Theory Application to the Physics of Condensed Matter* (Springer, 2008).
- [21] M. Dzero, K. Sun, P. Coleman, and V. Galitski, arXiv: cond-mat/1108.3371v1 (2011).
- [22] H. Zhang, C.-X. Liu, X.-L. Qi, X. Dai, Z. Fang, and S.-C. Zhang, Nat. Phys. **5**, 438 (2009).
- [23] L. Fu, C. L. Kane, and E. J. Mele, Phys. Rev. Lett. **98**, 106803 (2007).
- [24] J. M. Luttinger, Phys. Rev. **102**, 1030 (1956).
- [25] See supporting material.
- [26] N. Marzari and D. Vanderbilt, Phys. Rev. B **56**, 12847 (1997).
- [27] I. Souza, N. Marzari, and D. Vanderbilt, Phys. Rev. B **65**, 035109 (2001).